Available online at www.sciencedirect.com
ScienceDirect
Journal of Organometallic Chemistry 693 (2008) 1005–1019
Journal of Organometallic Chemistry
www.elsevier.com/locate/jorganchem

Complexation of tris(pentafluorophenyl)silanes with neutral Lewis bases

Alexander D. Dilman [a,*], Vitalij V. Levin [a], Alexander A. Korlyukov [b,*], Pavel A. Belyakov [a], Marina I. Struchkova [a], Mikhail Yu. Antipin [b], Vladimir A. Tartakovsky [a]

[a] *N.D. Zelinsky Institute of Organic Chemistry, Leninsky Prosp. 47, 119991 Moscow, Russian Federation*
[b] *A.N. Nesmeyanov Institute of Organoelement Compounds, Vavilov Str. 28, 119991 Moscow, Russian Federation*

Received 7 November 2007; received in revised form 6 December 2007; accepted 18 December 2007
Available online 28 December 2007

Abstract

A detailed analysis of monodentate and bidentate complexation of tris(pentafluorophenyl)silyl (TPFS) derivatives with neutral Lewis bases was performed. The NMR spectroscopy and X-ray diffraction analysis (11 structures) were the key methods to characterize tetra- or pentacoordinate silicon compounds, whereas the peculiarities of crystal packing were analyzed by means of DFT calculations. The interaction of TPFS-X (X = F, Cl, OTf) with strong Lewis bases (HMPA, *N*-methylpyrrolidinone) may afford three different species: neutral pentacoordinate TPFS(X)-L, cationic tetracoordinate TPFS-L^+ X^-, and cationic pentacoordinate TPFS-$(L)_2^+X^-$, representatives of each type were characterized by X-ray diffraction. A variety of complexes with bidentate complexation, featuring the trigonal bipyramidal geometry with apical C_6F_5-group was prepared and structurally characterized. The extent of Si–C_{apical} bond elongation depends on the donating ability of the coordinating ligand, with the longest Si–C bond of 1.981(1) Å observed for six-membered complex of TPFS-ether of *N*-(2-hydroxybenzoyl)pyrrolidine.

Keywords: Organosilicon chemistry; Tris(pentafluorophenyl)silyl derivatives; Hypervalent complexes; Structural studies

1. Introduction

The ability of silicon to expand its valence shell to form penta- and hexacoordinate species constitutes the key feature of organosilicon compounds, and the stability of hypercoordinate state increases with increasing the number of electron withdrawing groups [1]. The compounds bearing three heteroatomic substituents ($RSiX_3$, X = Hal, OR′) are able to interact with a wide variety of Lewis bases. On the contrary, trialkyl and triarylsilanes form pentacoordinate complexes either with strongly nucleophilic anionic Lewis bases [2] or upon bidentate coordination [3].

The pentafluorophenyl group occupies intermediate position between heteroatomic and alkyl groups, since it serves as electron depleting substituent while being at the same time sterically demanding carbon-centered fragment.

Recently, we found that tris(pentafluorophenyl)silyl (TPFS) derivatives can be employed as nucleophilic reagents in a number of C–C bond forming process, which proceed through the intermediacy of hypercoordinate complexes generated under very mild conditions [4]. Further support of strong influence of C_6F_5-group on energies of complexation of silanes with anionic Lewis bases was provided by quantum chemical calculations [4b].

These data prompted us to propose that, despite its significant steric bulk, TPFS-group would be able to interact with neutral Lewis bases leading to stable pentacoordinate complexes. Herein, we present the results of investigation of the coordinating properties of TPFS-derivatives towards monodentate and bidentate complexation. The interaction of Lewis bases with silicon was studied by means of NMR spectroscopy and X-ray diffraction analysis.

* Corresponding authors. Tel.: +7 495 137 68 29; fax: +7 499 135 53 28.
E-mail addresses: adil25@mail.ru (A.D. Dilman), alex@xrlab.ineos.ac.ru (A.A. Korlyukov).

0022-328X/$ - see front matter © 2007 Elsevier B.V. All rights reserved.
doi:10.1016/j.jorganchem.2007.12.022

2. Results and discussion

2.1. Monodentate coordination

2.1.1. NMR studies

Three different species may be formed upon interaction of TPFS-derivatives with Lewis bases (Scheme 1). The initial associative interaction affords pentacoordinate complex **1**, which may dissociate into cationic tetracoordinate silane **2**. The latter species may react with another molecule of Lewis base to provide positively charged pentacoordinate complex **3**. The formation of hexacoordinate complexes seems unlikely owing to the significant steric bulk provided by three C_6F_5-groups.

A series of TPFS-derivatives was considered, including silanes with methoxy-, fluoro-, chloro-, and triflate groups. For comparison, it was also interesting to test the silane with all carbon substituents, TPFS-Me. As Lewis bases, hexamethylphosphoric acid triamide (HMPA), *N*-methylpyrrolidinone (NMP) and pyridine were selected, and their affinity towards silicon increases in the following order: pyridine, NMP, HMPA [5]. The interaction of a silane with a Lewis base taken in a 1:1 ratio was studied in $CDCl_3$ solution at room temperature. The samples were routinely monitored by ^1H and ^{19}F spectroscopy, and whenever possible ^{13}C and ^{29}Si data were obtained.

No complexation of TPFS-Me and TPFS-OMe with Lewis bases was noted by ^1H and ^{19}F NMR data. Such a result for TPFS-Me was, in fact, expected, since in this molecule silicon does not have adjacent heteroatom. At the same time, the failure to observe complexation with TPFS-OMe was less anticipated. To gain more decisive evidence for the absence of complexation, the ^{29}Si NMR spectrum of TPFS-OMe in the presence of the strongest Lewis base HMPA was recorded, which showed no change relative to the reference spectrum of TPFS-OMe (−32.93 ppm).

Then we tuned our attention to more electrophilic silanes TPFS-F and TPFS-Cl. The combination of TPFS-F and TPFS-Cl with HMPA provided crystalline precipitates of compounds **1a**,**b** (Eq. (1)), and their structures were confirmed by single crystal X-ray diffraction analysis (*vide infra*). In case of adduct **1a** the complexation is evidenced by ^{19}F NMR data, where the signal of fluorine bound to silicon appeared 5.6 ppm downfield relative to that of uncomplexed TPFS-F. For complex **1b**, the only indication of complexation is a slight (1–2 ppm) upfield shift of signals of fluorine atoms with respect to TPFS-Cl. In ^1H spectra of **1a**,**b** the signal of dimethylamino groups was almost identical with that of authentic HMPA. Unfortunately, we have not been able to measure ^{13}C and ^{29}Si NMR spectra of **1a**,**b** owing to their low solubility.

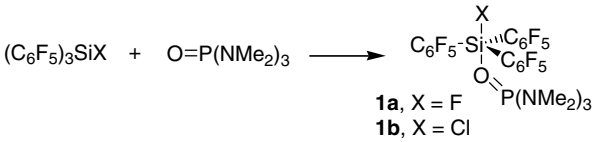

(1)

A mixture of TPFS-F and NMP provided interesting results. While virtually no change was noted in proton spectrum of Lewis base, in ^{19}F spectrum the signal of fluorine connected to silicon was significantly broadened and shifted a little downfield (about 1.0 ppm relative to uncomplexed silane). At the same time no signal appeared in ^{29}Si spectrum, presumably due to line broadening. These data suggest that a rapid and reversible interaction of TPFS-F and NMP takes place (Eq. (2)). Attempts to shift the equilibrium towards pentacoordinate species **1c** using three equivalents of NMP were unsuccessful. When a mixture of TPFS-Cl and NMP was studied by ^1H, ^{19}F, and ^{29}Si NMR spectroscopy, no complexation was noted.

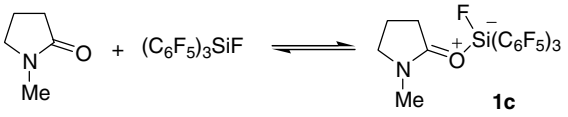

(2)

Surprisingly, no complexation between silanes TPFS-X (X = F, Cl) and pyridine was observed. Given that silicon tetrafluoride and tetrachloride are known to form stable adducts with pyridine [6], and taking into account our quantum chemical data suggesting the stronger stabilizing effect of C_6F_5-group relative to that of halogen [4b], the lack of complexation of TPFS-F and TPFS-Cl may be associated with steric bulk of C_6F_5-group.

Finally, the behavior of the most reactive silane, TPFS-OTf, was investigated. Silyltriflates are known to be highly electrophilic species serving as powerful silylating reagents [7] and as Lewis acids [8]. For example, trimethylsilyl triflate (TMSOTf) readily transfers Me_3Si-group onto a variety of Lewis basic molecules such as pyridines, amides, and

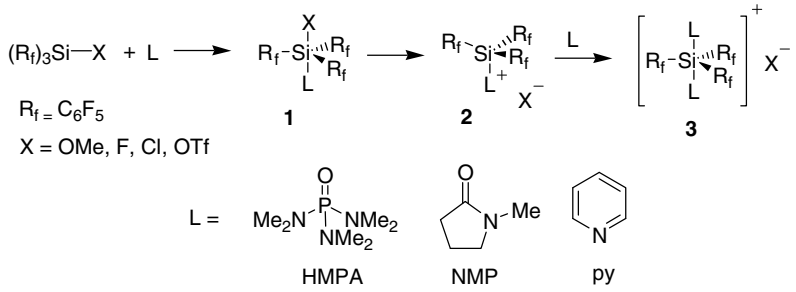

Scheme 1.

phosphineoxides (Ph_3PO, HMPA) to afford tetracoordinate salts $Me_3Si–L^+$ OTf^- [5,9].

When we mixed TPFS-OTf with 1 equiv. of HMPA in $CDCl_3$ the formation of precipitate was observed. Its structure was determined by X-ray diffraction to contain ionic complex **3a** with two molecules of HMPA and dissociated triflate anion (Eq. (3)). The very low solubility of **3a** hampered its NMR characterization.

Fortunately, no solubility problems were encountered for the pair TPFS-OTf and NMP. In this case the nature of the complex observed depends on the ratio of the reagents. Thus, for 1:1 mixture the cationic tetracoordinate complex **2b** was the only species observed by ^1H, ^{19}F, ^{13}C and ^{29}Si NMR, and its structure was proven by X-ray diffraction. Addition of second equivalent of NMP induced the formation of pentacoordinate complex **3b**, that can be supported by the following data: (a) the ^{29}Si signal −49.67 ppm, which is shifted upfield relative to those of TPFS-OTf (−26.53) and **2b** (−25.85); (b) the signals in ^1H spectrum of **3b** appear intermediate between those of uncomplexed NMP and **2b** (Fig. 1).

Addition of third equivalent of NMP provides only one set of pyrrolidinone signals in proton spectrum, which is intermediate between those of **3b** and uncomplexed NMP, suggesting that in this system the rapid equilibrium processes are taking place. In ^{29}Si spectrum, only one signal at −51.03 ppm was observed. The insignificant difference of ^{29}Si chemical shifts between 3:1 and 2:1 NMP/TPFS-OTf ratios supports the conclusion that even at 2:1 ratio, complex **3b** is the major component of the equilibrium mixture. Furthermore, this result testifies against the formation of hexacoordinate species, for which the upfield shift in ^{29}Si NMR could be expected.

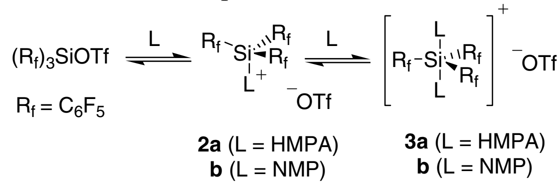

(3)

It was surprising to find that TPFS-OTf and pyridine showed no signs of complexation, as evidenced by ^1H and ^{19}F NMR spectroscopy. At the same time, earlier we noted that pyridine may catalyze the silylation reaction using TPFS-OTf [10]. These data can be explained by fast reversible interaction of TPFS-OTf with pyridine, with the equilibrium being strongly shifted to the starting components. The reluctance of pyridine to afford stable complex with TPFS-OTf may be attributed to steric effect of TPFS-group.

2.1.2. Structural studies

The structures of neutral HMPA complexes **1a**,**b** derived from X-ray diffraction analysis are shown in Figs. 2 and 3, Table 1. The structures of starting TPFS-F and TPFS-Cl

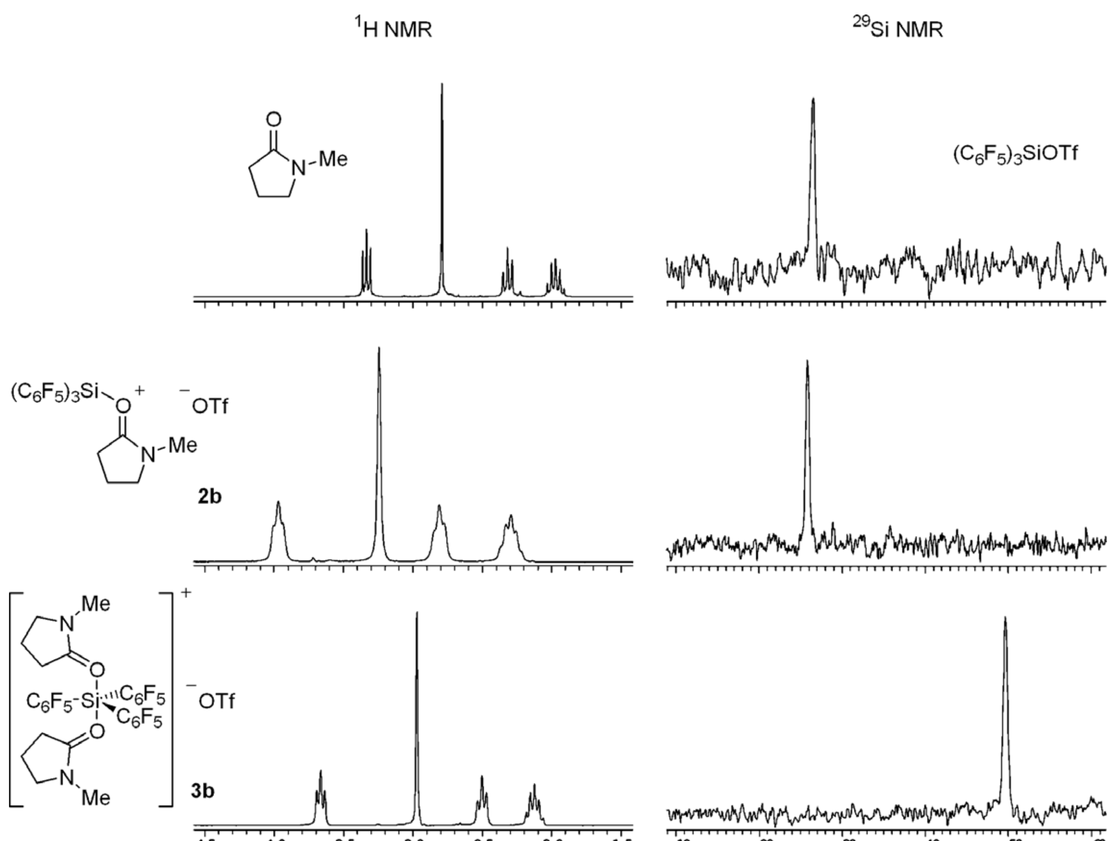

Fig. 1. ^1H NMR (left) and ^{29}Si NMR (right) spectra of complexation of NMP with TPFS-OTf in $CDCl_3$ at room temperature.

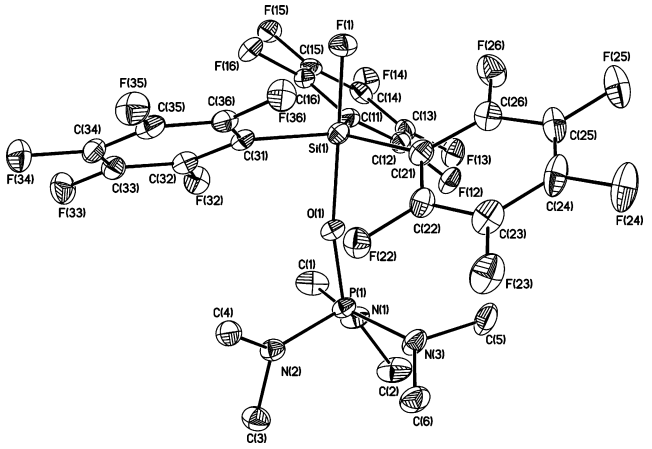

Fig. 2. Molecular structure of **1a** presented by thermal ellipsoids at 50% probability.

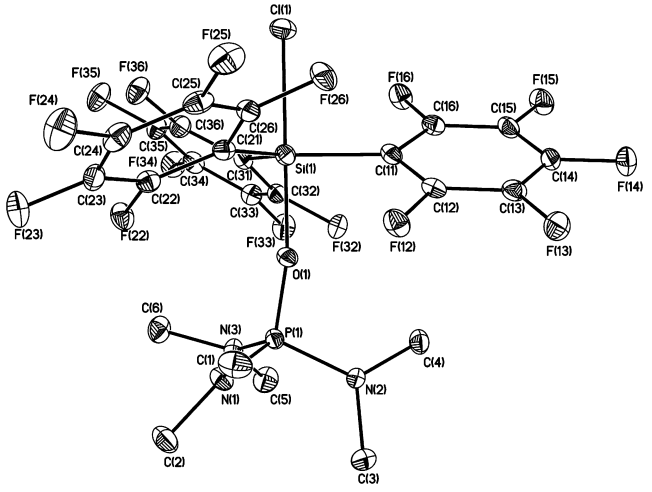

Fig. 3. Molecular structure of **1b** presented by thermal ellipsoids at 50% probability.

were also determined for comparison (Table 1). It should be pointed out, that in the literature only two compounds containing pentacoordinate complexes of silanes with phosphine oxides are described [11]. There are also several tetracoordinate structures containing Si-HMPA fragment, in which silicon atom is a part of metal silylene moiety [12–15].

Complexes **1a**,**b** possess rather strong interaction between TPFS-fragment and HMPA, that is reflected by Si–O bond lengths which are only by 0.17–0.22 Å longer than standard value for covalent Si–O bonds [16]. The coordination polyhedron of Si atom can be described as almost ideal trigonal bipyramid with deviation of Si atom from plane of three equatorial carbon atoms (Δ_{Si}) of 0.06 and 0.003 Å in **1a** and **1b**, respectively. Such a fact is surprising taking into account the high steric crowding of silicon coordination center. Indeed, the HMPA and $Si(C_6F_5)_3$ moieties in **1a**,**b** are in unfavorable eclipsed conformation (pseudotorsional angles N(3)P(1)Si(1)C(21) and N(2)P(1)Si(1)C(11) are equal to 4.1° and 4.7° in **1a** and **1b**, respectively).

The comparison of Si–F bond length in **1a** with that in uncomplexed TPFS-F revealed the elongation by 0.07 Å upon complex formation. The interaction of TPFS-Cl with HMPA results in more pronounced Si–Cl bond elongation (ca. 0.20 Å), thereby supporting the notion of higher sensitivity of Si–Cl vs. Si–F bond towards additional coordination [17].

It is also interesting to consider the value of Si–O–P angle and compare it with literature data. Thus, in the case of **1a**,**b** the Si–O–P angles are close to linear (166.9° and 165.2°, respectively). In general, M–O–P (M = metal) angles in HMPA complexes vary in range 142–165°, the largest magnitudes were observed in complexes with lantanides and actinides [18]. Concerning the literature examples of Si-HMPA derivatives, the Si atoms always adopt the

Table 1
Principal structural parameters of complexes **1a**,**b**, **2b**, **3a**, TPFS-F, and TPFS-Cl

	Parameters obtained by X-ray diffraction						Parameters calculated by PW-PBE		
	1a	**1b**	**2b**[a]	**3a**	TPFS-F	TPFS-Cl	**1a**	**1b**	**3a**
Si(1)–Hal(1)	1.656(1)	2.2472(8)			1.585(1)	2.0399(9)	1.692	2.257	
Si(1)–O(1)	1.871(2)	1.824(1)	1.662(1)	1.795(1)			1.883	1.846	1.816
				1.837(1)					1.863
Si(1)–C(11)	1.901(2)	1.895(2)	1.862(2)	1.896(2)	1.868(2)	1.869(2)	1.914	1.909	1.910
Si(1)–C(21)	1.892(2)	1.897(2)	1.862(2)	1.897(2)	1.865(2)	1.867(2)	1.918	1.912	1.910
Si(1)–C(31)	1.902(2)	1.901(2)	1.864(2)	1.897(2)	1.861(2)	1.871(2)	1.913	1.914	1.909
P(1)–O(1)	1.511(2)	1.519(1)		1.523(1)			1.528	1.534	1.538
				1.518(1)					1.533
P–N (on average)	1.628(2)	1.627(1)		1.628(1)			1.644	1.642	1.642
O–Si–Hal	179.44(8)	179.92(7)					179.2	179.6	177.7
O–Si–O				178.30(6)					
C(11)–Si(1)–C(21)	121.23(9)	118.80(9)	113.35(9)	119.98(7)	111.84(8)	113.27(8)	121.5	118.6	119.8
C(11)–Si(1)–C(31)	119.37(9)	119.05(9)	110.4(1)	120.87(7)	112.26(7)	113.39(8)	119.2	119.0	121.1
C(21)–Si(1)–C(31)	119.14(9)	122.15(9)	110.21(9)	119.10(7)	112.90(7)	106.24(8)	119.1	122.5	118.7
P(1)–O(1)–Si(1)	166.9(1)	165.16(9)		177.27(8)			166.4	164.7	177.7
				169.13(8)					168.7
Δ_{Si}	0.06(1)	0.004(1)		0.00241(9)			0.05	0.001	0.0024

[a] The averaged values of two independent molecules are given.

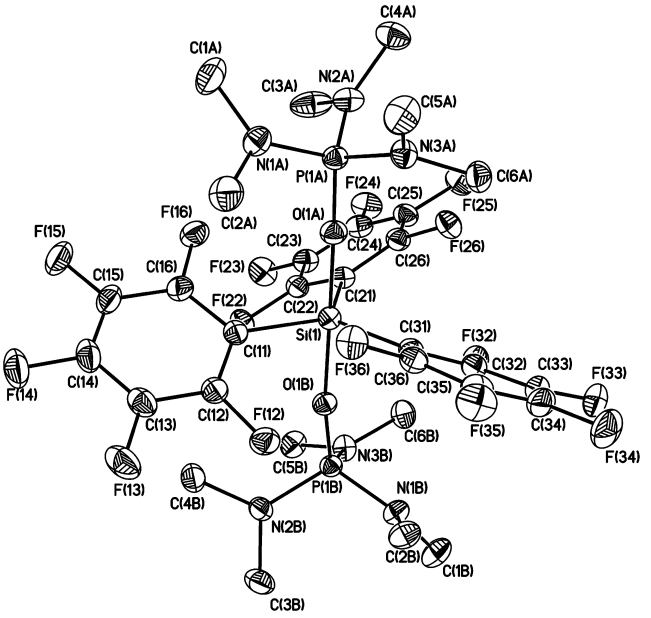

Fig. 4. Molecular structure of **3a** presented by thermal ellipsoids at 50% probability. Triflate anion is omitted for clarity.

slightly distorted tetrahedral configuration with the Si–O–P angle not exceeding 153° [the Si–O bonds are close to the standard values (1.69–1.74 Å)] [12–15]. Almost the same value for Si–O–P angle is observed in neutral complexes with square-pyramidal Si atom containing $O{=}P(N(CH_2)_4)_3$ and $O{=}PPh_3$ (144.3° and 143.2°, respectively) [11].

The cationic complex **3a** containing two HMPA molecules is presented in Fig. 4. It is the first example of acyclic trigonal-bipyramidal organosilicon cations with O–Si coordination characterized by X-ray diffraction. Indeed, structural data for pentacoordinated acyclic complexes are limited to only two species with Si–N coordination [19], whereas many other cationic silicon complexes are tetracoordinated [18].

The coordination polyhedron of Si atom can be described as almost ideal trigonal bipyramid (O(1A)Si(1)O(1B) angle is equal to 178.30(6)° and Δ_{Si} is 0.02 Å toward the O(1B) atom). The Si(1)–O(1A) and Si(1)–O(1B) bonds differ by 0.04 Å which can be explained by the influence of crystal packing. Similar to **1a**,**b**, in **3a** the molecules of HMPA and $Si(C_6F_5)_3$ moiety are arranged in eclipsed conformation (the pseudotorsional angles N(1A)P(1A)Si(1)C(11) and N(2B)P(2B)Si(1)C(11) are equal to 0.73° and −57°, respectively), and the Si–O–P angles are close to linear (169.1° and 177.3°). In the crystal of **3a** the triflate anion does not have any influence on the geometry of the cation, since the shortest Si···OTf distance of 6.22 Å is far beyond the sum of the Van der Waals radii (3.5 Å).

Probably, the stability of HMPA complexes **1a**,**b** and **3a** is associated with strong electron deficient character of $Si(C_6F_5)_3$ fragment, that overwhelms the steric effects. Given that the studied complexes have nearly the same structure of Si coordination polyhedron, one can propose that their energies of Si–O coordination are of similar order. The information about the energy of Si–O coordination would be useful for estimation of relative stability of acyclic complexes containing $Si(C_6F_5)_3$ moiety. Though this issue would be best treated by *ab initio* quantum chemical calculations, the optimization of atomic position in good level of theory for systems containing 100 atoms (as in **3a**) is problematic at present. Furthermore, analysis of literature concerning pentacoordinated silicon species has shown that interatomic Si–O distances in isolated molecules [20,21] in most cases exceed the experimental values (revealed by X-ray diffraction) by 0.2–0.3 Å, that makes difficult direct comparison of theoretical and experimental results.

In order to mimic the electronic structure of **1a**,**b** and **3a** in crystal we carried out the quantum chemical calculation in terms of DFT theory (PBE exchange-correlation functional) of these crystal structures using plane wave (PW) basis sets for valence and semi-core electrons and projector augmented waves (PAW) formalism for description of core electron. The optimization of atomic positions led to slight elongation (by ca. 0.02 Å) of all bonds formed by Si atom. The elongation of P(1)–O(1) and C–F bonds have nearly the same magnitude. The most pronounced discrepancies are observed for intermolecular H···F contacts (<0.1 Å, on average). The reason of such differences is errors of DFT theory in description of weak interatomic interactions. Using PBE functional allowed us to improve the reproduction of interatomic distances corresponding to the weak intermolecular contacts H···F in comparison with LDA functional. In general, the experimental and calculated crystal structures of **1a**,**b** and **3a** are in satisfactory agreement, so, the PW-PBE approach is a good choice for investigation of their electron structure.

Analysis of chemical bonding pattern in complexes under discussion was performed using topological analysis of calculated electron density function ($\rho(r)$) in terms of R.F. Bader's "Atom in molecules theory" (AIM) [22]. This theoretical approach allows one not only to determine chemical bonding type but also estimate the bond energy. Results of the topological analysis can be directly compared with experimental charge density studies of penta- and hexacoordinated organosilicon compounds [21,23,24].

The peculiarities of chemical bonding in coordination center of Si atom are illustrated by section of deformation electron density (DED) (Figs. 5 and 6). Both in neutral molecules **1a**,**b** and in cation **3a** in the region of Si–O and Si–Hal bonds the maxima of electron density are observed. These maxima are shifted toward O and Hal atoms and localized at 0.5–0.7 Å from them. Topological analysis of $\rho(r)$ have shown that critical points (CP) (3, −1) are found for all chemical bonds including coordination Si–O ones, as well as for weak intermolecular H···F, O···H and F···F interactions. The characteristics of H···F and F···F intermolecular interactions in crystals of TPFS derivatives $(C_6F_5)_3SiNR_2$ were studied in terms of AIM theory and published previously [25].

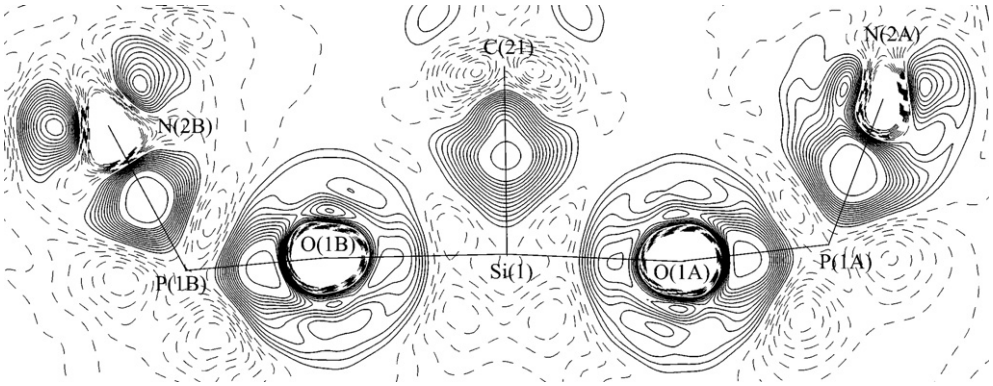

Fig. 5. Section of deformation electron density of **3a** in plane O(1A)Si(1)C(21). Contours are drawn through 0.02 e Å^{-3}. Negative values are shown by dashed lines.

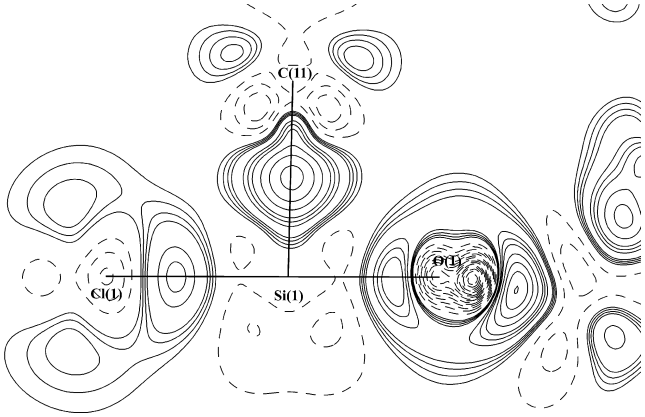

Fig. 6. Deformation electron density map of **1b** in O(1)–Si(1)–C(11) plane. Isolines are drawn through 0.02 e Å^{-3}, negative contours are dashed.

The bonds formed by Si and P atoms are characterized by positive values of Laplacian of electron density ($\nabla^2\rho(r)$) and negative ones of local energy density ($E^e(r)$) in CP(3, −1) that corresponds to intermediate type of interatomic interactions in terms of AIM theory [22]. The energy of Si–O coordination bonds was estimated using correlation proposed by Espinosa et al. [26]. Previously, we successfully utilized this approach for investigation of Si–O coordination bond in silylium ions and neutral compounds with coordination Si–O and Ge–O bonds [21,24,27].

It can be seen from Table 2 that values of Si–O bond energies in **1a**,**b** are sufficiently large (39.1 and 45.7 kcal/mol). Thus, the strength of coordination bonds can be responsible for the high stability of complexes **1a**,**b**. In cation **3a** the coordination Si(1)–O(1A) bond appears to be stronger than Si(1)–O(1B) (53.2 and 44.1 kcal/mol, respectively). Such a difference can be explained by influence of crystal packing. Actually, two formally the same HMPA ligands form non-equivalent systems of intermolecular contacts. The summation of contacts energies for HMPA ligands labeled A and B separately gave 39.2 and 36.7 kcal/mol. So, the difference in total contact energy is comparable with that for Si(1)–O(1A) and Si(1)–O(1B) bonds. It is interesting to note that sum of energies of Si(1)–O(1A) and Si(1)–O(1B) bonds is 97.3 kcal/mol that is very close to the standard value for Si–O bond energy (100–120 kcal/mol). The latter fact is in good agreement with theory of hypervalent bonding that predicts the closeness of bond orders of apical bonds in the case of three centered four electron (3c-4e) interaction [28]. Thus, one may conclude that stabilization of cation **3a** is caused by presence of 3c–4e interaction in O–Si–O fragment.

The crystal of tetracoordinate cationic complex **2b** containing NMP ligand has two independent molecules (Fig. 7, Table 1). In these molecules, the silicon atom has distorted tetrahedral configuration with slightly different Si(1)–O(1) and Si(1′)–O(1′) bond lengths (1.652(2) and 1.672(2) Å, respectively). Such a difference can be related with peculiarities of cation–anion interactions in crystal of **2b**. Thus, two independent triflate anions are located nearby the Si(1) atom with the interatomic Si(1)–O(3T) and Si(1)–O(5T) distances of 3.716 and 3.497 Å, that is close to the sum of the Van der Waals radii.

In complex **2b**, the positive charge is delocalized between oxygen and nitrogen atoms of amide fragment. Indeed, the C(1)–N(1) bond is shorter by ca. 0.05 Å and C(1)–O(1) is longer by ca. 0.08 Å than similar bonds in uncomplexed pyrrolidinone derivatives [18].

2.2. Bidentate coordination

The key feature of monodentate pentacoordinate complexes described in the previous section is that two heteroatom substituents around silicon occupy apical positions. Linking two Lewis basic fragments within one molecule would allow to observe structures, in which one heteroatomic group would be located in apical and the other in equatorial positions. Consequently, one C_6F_5-group will be forced to occupy apical orientation.

In analogy to the equation presented in Scheme 1, two different modes for the bidentate complexation can be formulated (Scheme 2). The interaction of silyl ether fragment with basic moiety provides neutral pentacoordinate species, while the cationic complex could be obtained if bidentate

Table 2
Topological characteristics and related bond energies of selected bonds in complexes **1a**,**b**, **3a**, and **5**

Bond	**1a**	**1b**	**3a**	**5**
ρ(r) (e Å^{-3})				
Si(1)–O(1)	0.60	0.63	0.68	0.57
Si(1)–X[a]	0.92	0.52	0.60	1.01
Si(1)–C(11)	0.84	0.85	0.85	0.72
Si(1)–C(21)	0.83	0.85	0.85	0.83
Si(1)–C(31)	0.84	0.84	0.85	0.85
$\Delta^2\rho(r)$ *(e Å^{-5})*				
Si(1)–O(1)	9.02	10.46	12.72	7.54
Si(1)–X[a]	19.34	1.73	11.095	19.41
Si(1)–C(11)	2.49	2.05	2.82	1.31
Si(1)–C(21)	2.41	2.28	2.86	2.16
Si(1)–C(31)	2.39	2.21	2.81	2.53
$E^e(r)$ (*Hartree Å^{-3}*)				
Si(1)–O(1)	−0.10	−0.12602	−0.12702	−0.13944
Si(1)–X[a]	−0.24	−0.22784	−0.08648	−0.36979
Si(1)–C(11)	−0.54	−0.57	−0.53	−0.44
Si(1)–C(21)	−0.54	−0.55	−0.52	−0.56
Si(1)–C(31)	−0.55	−0.55	−0.53	−0.54
$V^e(r)$ *(a.u) [E_{bond} (kcallmol)]*				
Si(1)–O(1)	−0.125 [39.1]	−0.146 [45.7]	−0.170 [53.2]	−0.120 [37.5]
Si(1)–X[a]	−0.273 [85.4]	−0.085 [26.8]	−0.141 [44.1]	−0.311 [97.4]
Si(1)–C(11)	−0.187 [58.6]	−0.189 [59.3]	−0.196 [61.4]	−0.144 [45.0]
Si(1)–C(21)	−0.184 [57.7]	−0.187 [58.9]	−0.196 [61.4]	−0.191 [60.0]
Si(1)–C(31)	−0.187 [58.7]	−0.186 [58.4]	−0.196 [61.3]	−0.183 [57.3]

[a] X = F (for **1a**), Cl (for **1b**), O(1B) (for **3a**), O(2A) (for **5**).

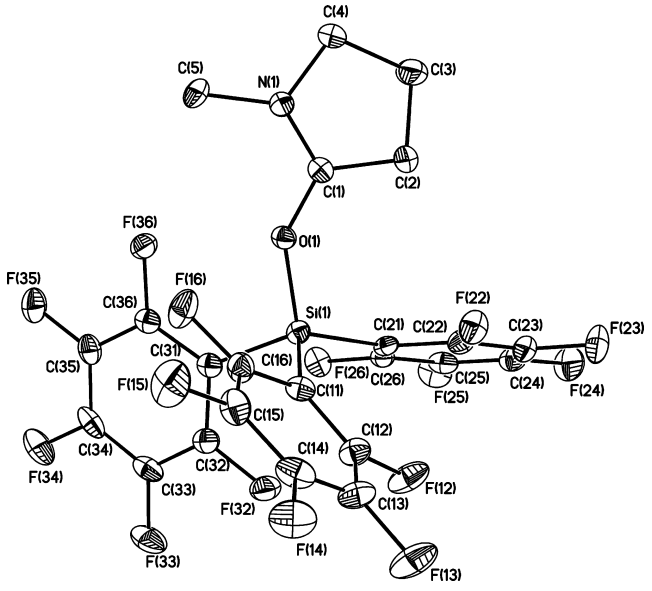

Fig. 7. Molecular structure of **2b** presented by thermal ellipsoids at 50% probability. Triflate anion is omitted for clarity.

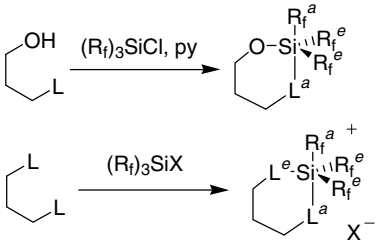

Scheme 2. Superscripts *a* and *e* correspond to apical and equatorial position.

Lewis base is combined with a silane possessing good leaving group.

There are several key structural parameters that provide meaningful information about the nature of the bidentate coordination: the coordination bond distance Si···L^a, the angle R$_f^a$–Si–L^a, and the distance between silicon and apical carbon (Si···R$_f^a$). The latter parameter seems to be the most characteristic concerning the strength of coordination bond, since it is known that apical bond experiences most notable elongation upon complexation.

A series of silyl ethers **4**–**6** were prepared by silylation of corresponding phenols with TPFS-Cl in the presence of pyridine or triethylamine (Chart 1). The ether **7** was synthesized by aldol coupling of 1-tris(pentafluorophenyl)silyloxycyclopentene with isobutyraldehyde. The strength of coordination bond can be analyzed by means of ^{29}Si NMR spectroscopy for compounds **4**, **6**, and **7**, while very low solubility of amide complex **5** rendered its characterization problematic. For the sake of comparison, the TPFS-ether of phenol was prepared, which is devoid of Lewis basic group. Since the increase of the field of the signal reflects the increase in pentacoordinate character, it can be proposed that the coordination becomes stronger in the order **4** < **7** < **6**. To gain further insight into structural

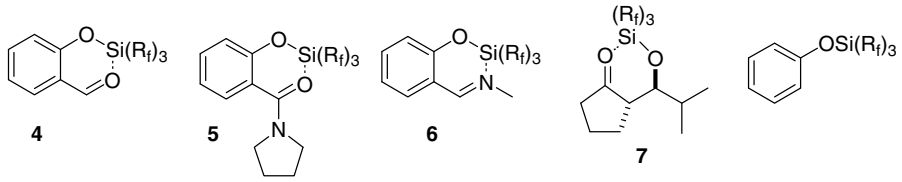

Chart 1.

features of compounds **4**–**7**, they were studied by X-ray diffraction analysis (Figs. 8–11, Table 3).

Compounds **4** and **7** contain weak coordination bond Si–O (2.831(2) and 2.784(2) Å, respectively), that is associated with well-known poor donating ability of aldehyde and ketone ligands towards silicon Lewis acids [29]. However, this interaction is sufficient to affect the coordination geometry with elongation of the apical Si(1)–C(11) bonds to 1.896 and 1.889(3) Å in **4** and **7**, respectively, that is by 0.02 Å longer compared to equatorial ones. The covalent Si(1)–O(2A) bonds are somewhat shorter than standard value (1.64 Å) due to electron-withdrawing effect of $Si(C_6F_5)_3$ moiety [30].

The introduction of donor pyrrolidine group at carbonyl atom (complex **5**) led to dramatic shortening of coordination Si···O distance to 1.9079(9) Å resulting in clear trigonal bipyramidal arrangement of silicon. The apical Si(1)–C(11) bond of 1.981(1) Å is significantly longer by ca. 0.11 Å than that in tetracoordinated TPFS-derivatives. However, such an elongation is slightly less than that in complexes with atrane-like cage structure having Si–N coordination bond (Si–C 1.996 Å) [31]. Interestingly,

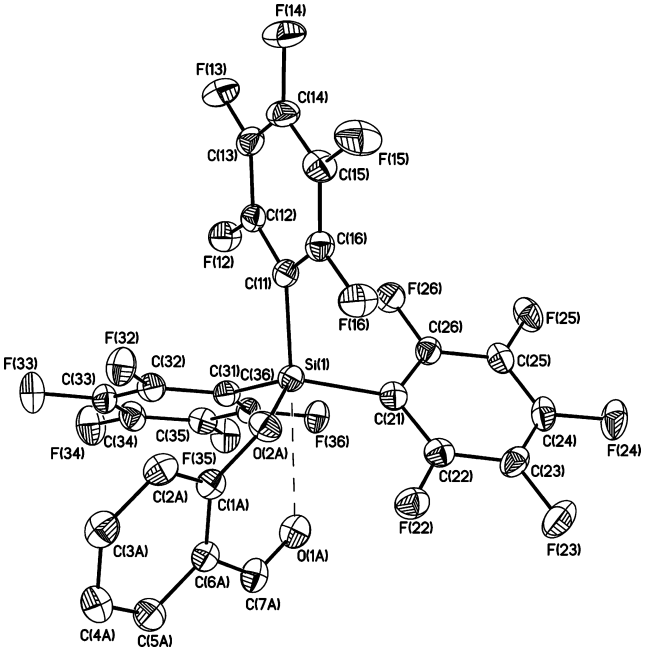

Fig. 8. Molecular structure of **4** presented by thermal ellipsoids at 50% probability.

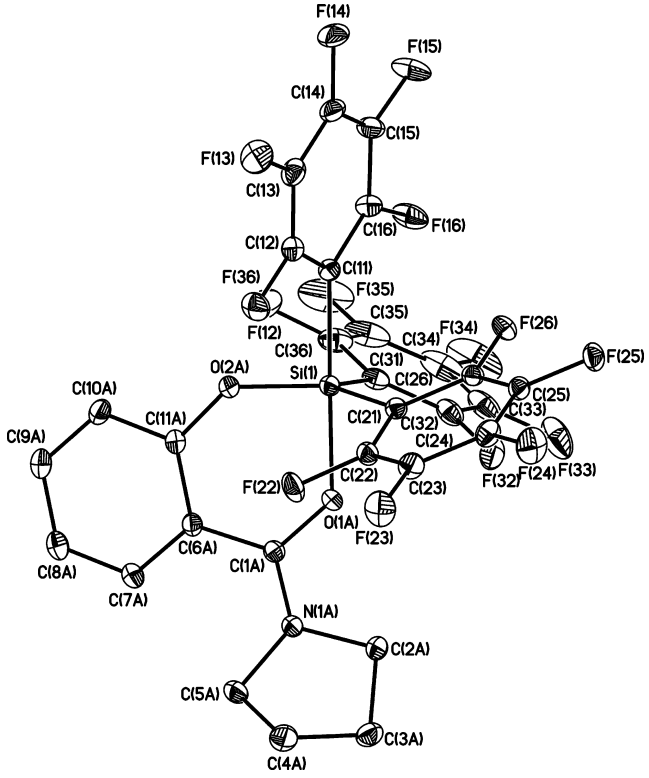

Fig. 9. Molecular structure of **5** presented by thermal ellipsoids at 50% probability.

though in the crystal structure of **5** C_6F_5-groups can be clearly denoted as apical and equatorial, in solution in ^{19}F NMR spectrum only one set of signals is observed, that may result from fast pseudorotation.

In complex **6** the apical bond distance Si(1)–C(11) of 1.9664(19) Å suggests that the Si–N coordination bond is quite strong, though it is somewhat weaker than Si···O interaction in complex **5**. In complex **6**, the silicon atom has trigonal bipyramidal geometry with Si–N distance of 2.123(2) Å which is by 0.27 Å longer than standard value of covalent Si–N bond [16]. It is worthy of note that the decrease of the length of coordination bond Si···L in the order **4** > **6** > **5** is accompanied by the decrease of the angle R_f^a–Si–L (**4**, 178.1°; **6**, 174.7°; **5**, 172.1°). This trend allows one to conclude that steric hindrance is rising along with the strengthening of coordination bond.

In general, the presence of bidentate coordination led to pronounced bending of apical C_6F_5 groups from the lines of Si(1)–C(11), Si(1)–C(21) and Si(1)–C(31) bonds. Indeed,

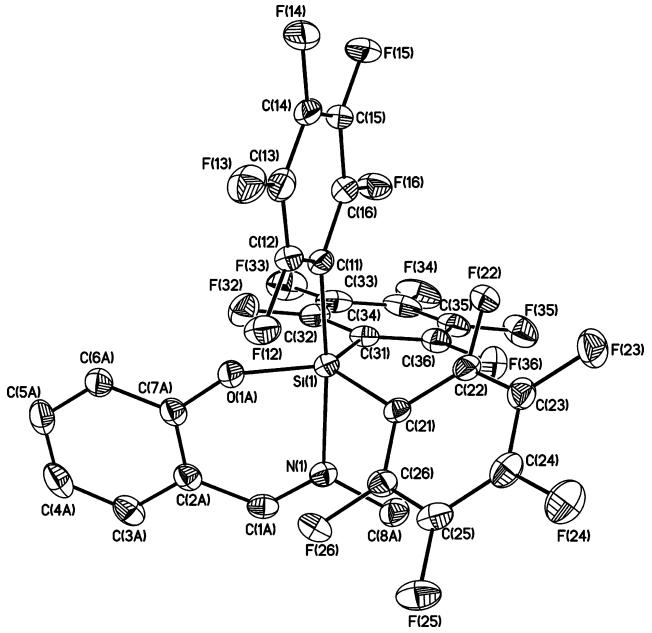

Fig. 10. Molecular structure of **6** presented by thermal ellipsoids at 50% probability.

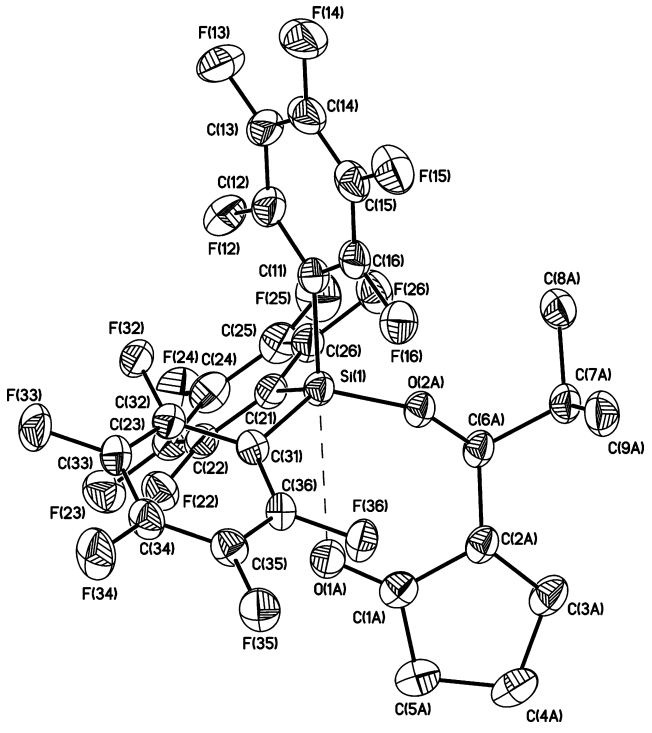

Fig. 11. Molecular structure of **7** presented by thermal ellipsoids at 50% probability.

the averaged values of bending angles in **5** and **6** are equal to 6.8° while in acyclic complexes varies in range 1.5–4.5°. However in TPFS-Cl one bending angle (8.5°) is even larger than in the case of **5** and **6**. The most probable reason of such pronounced bending in TPFS-Cl is inter- and intramolecular F···F and C···F contacts.

To estimate the energy characteristics the quantum chemical calculation of crystal packing of complex **5** has been performed. The level of theory used was the same as for **1a**,**b** and **3a**.

Structural parameters of silicon atom in **5** are close to experimental with theoretical values of Si–O and Si–C bonds being longer by 0.01–0.02 Å. The elongation of Si(1)–C(11) compared to Si(1)–C(21) and Si(1)–C(31) bond does not lead to significant change of electron density distribution in region of apical fragment O–Si–C (Fig. 12).

The energy of coordination Si–O bond in **5** (37.5 kcal/mol) is somewhat decreased in comparison with acyclic complexes **1a**,**b** and **3a** but it is significantly stronger than Si–O bonds in pentacoordinated monochelate complexes previously studied in terms of AIM theory [23,24,27]. Due to highly covalent nature of Si–C bonds the estimation of their energies using correlation scheme described in the literature [26] can be not so reliable as in the case of Si–O bonds. According to literature data the energy of Si–C bond in poly(dimethylsiloxane) (Si–C bond length is 1.85 Å) is equal to 85 kcal/mol [32]. So, the energies of equatorial Si–C bonds calculated from those topological characteristics (60.0 and 57.3 kcal/mol) are in good agreement with values obtained for poly(dimethylsiloxane) taking into account the considerable elongation of Si–C bond (ca. 0.06 Å) in complex **5**. Thus, the apical Si(1)–C(11) bond is weakened by 13–15 kcal/mol as compared to equatorial Si–C bonds (Table 2). The "weak" Si(1)–C(11) bond clearly shows that C_6F_5 moiety is a "good" leaving group in S_N2 reactions at pentacoordinated silicon atom.

As the bidentate Lewis base, we employed the pyrrolidine diamide of succinic acid (**8**). When the diamide **8** was mixed with TPFS-OTf the formation of precipitate occurred (Eq. (4)). This product was analyzed by ^{1}H, ^{19}F, and ^{13}C NMR spectroscopy and by X-ray diffraction analysis, which revealed the expected seven-membered cyclic structure **9** (Fig. 13, Table 3)

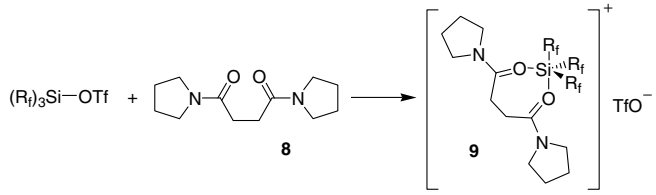

(4)

Analysis of Cambridge data base showed that **9** is the first example of cationic monochelate complexes of pentacoordinated silicon with seven-membered chelate cycle, while most of structurally characterized cationic complexes have five- or six-membered bis-chelate structures.

The crystal structure of cationic complex **9** contains two independent cations, in which the apical Si···O interatomic distance differs by 0.25 Å! This phenomenon may be associated with flexibility of seven-membered cycle. Notably,

Table 3
Principal structural parameters (Å and °) of complexes **4**–**7** and **9**

	4	**5**	**6**[a]	**7**	**9**[b]
Si(1)–O(1A)	2.831(2)	1.9079(9) [1.915]	1.6549(14)	2.784(2)	2.128(4) 2.367(4)
Si(1)–O(2A)	1.620(2)	1.6660(9) [1.689]	2.1230(2)	1.602(1)	1.689(4) 1.664(4)
Si(1)–C(11)	1.889(3)	1.981(1) [1.991]	1.966(2)	1.896(2)	1.946(7) 1.930(7)
Si(1)–C(21)	1.875(3)	1.905(1) [1.921]	1.904(2)	1.873(2)	1.871(6)
Si(1)–C(31)	1.872(3)	1.893(1) [1.907]	1.910(2)	1.878(2)	1.862(6)
O(1A)–C	1.211(3)	1.282(1) [1.294]	1.348(2)	1.210(2)	1.256(7)
O(2A)–C	1.366(3)	1.361(1) [1.356]	1.282(2)	1.435(2)	1.322(6)
O(1A)–Si(1)–C(11)	178.1(1)	172.13(4) [171.4]	174.67(8)	175.57(8)	174.3(2) 174.8(3)
O(1A)–Si(2)–O(2A)	74.3(1)	90.71(4) [90.8]	87.04(6)	76.46(6)	83.2(2)
C(11)–Si(1)–C(21)	105.13(12)	89.25(5) [88.9]	92.85(8)	109.8(1)	96.7(3)
C(11)–Si(1)–C(31)	108.53(12)	100.46(5) [100.7]	101.48(8)	100.40(9)	103.9(4)
C(21)–Si(1)–C(31)	116.21(12)	120.28(5) [121.4]	120.00(8)	112.93(9)	120.4(3)
Δ_{Si}	0.492(2)	0.0987(6) [0.096]	0.133(1)	0.440(1)	0.204(3) 0.315(4)

PW-PBE calculated values are placed in square brackets.
[a] The values for N(1)–C(1) bond, as well as N(1)–Si(1)–C(11) and N(1)–Si(2)–O(1A) bond angles, are given.
[b] Either values of two independent molecules or averaged values are given.

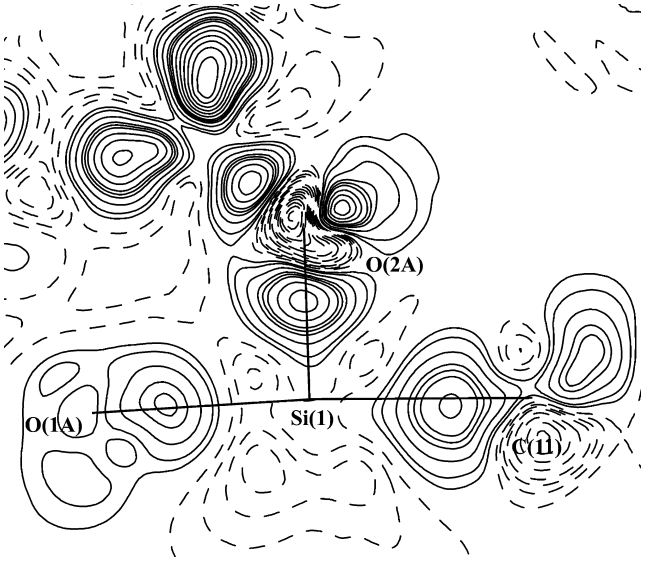

Fig. 12. Deformation electron density map of **5** in O(1A)–Si(1)–(O2A) plane. Isolines are drawn through 0.02 e Å^{-3}, negative contours are dashed.

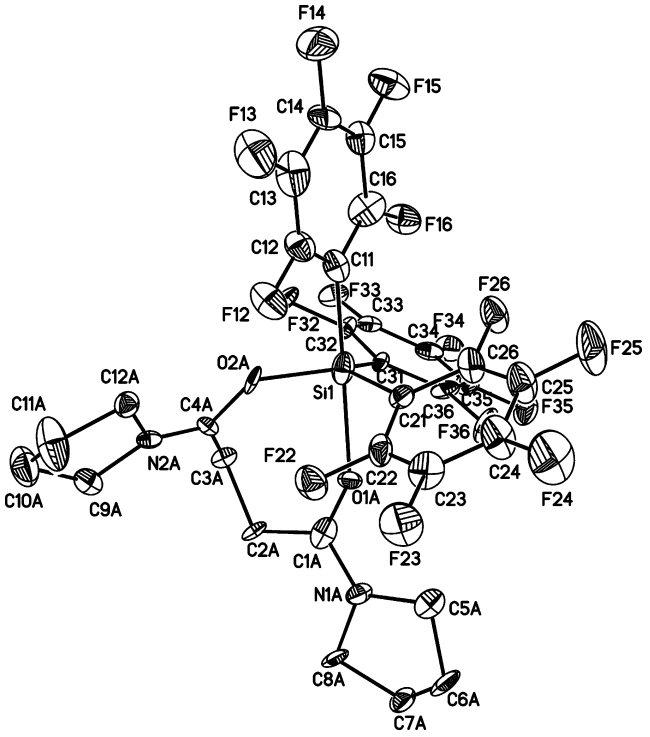

Fig. 13. Molecular structure of **9** with shortest Si–O bond presented by thermal ellipsoids at 50% probability. Triflate anion is omitted for clarity.

the molecule with shorter Si···O bond possesses longer Si···C_6F_5 bond meaning that these two species serve as a model for the complexation event.

It is worthy of note, that in ^{1}H NMR spectrum of complex **9** in $CDCl_3$ solution at room temperature two pyrrolidine fragments are identical. The rapid exchange of amide groups can occur either by rupture and formation of the Si–O bond, or through the pseudoration in pentacoordinate state.

3. Conclusion

We demonstrated that TPFS-derivatives bearing at silicon heteroatomic group may interact with sterically non-hindered Lewis bases to form neutral or cationic

penta- or tetracoordinate complexes. The neutral pentacoordinate species are formed in case of fluoro- and chloro silanes, whereas silyl triflate provides only cationic complexes. In the latter case, it was shown that by using moderately donating Lewis base such as *N*-methylpyrrolidinone the coordination state can be controlled by the stoichiometry between the silane and the Lewis base.

In contrast to monodentate complexation, the bidentate coordination involving TPFS-fragment can be achieved much more easily leading to the structures with apical C_6F_5-group. The extent of Si–C_{apical} bond elongation depends on the donating ability of the basic moiety, which can vary from poorly basic aldehyde carbonyl to strongly nucleophilic amide group.

4. Experimental

Silanes TPFS-Cl [33], TPFS-F [4b], TPFS-OTf [34], *N*-(2-hydroxybenzoyl)pyrrolidinone [35], *N*-methyl-*N*-[2-hydroxybenzyliden]amine [36], 1-tris(pentafluorophenyl)silyloxycyclopentene [34], and amide **8** [37] were synthesized according to the literature procedures. HMPA and NMP were distilled in vacuum from CaH_2 and stored under argon over MS 4A. All NMR measurements were carried out in $CDCl_3$ which was distilled from CaH_2 and stored over MS 4A. Melting points were determined in a sealed capillary.

4.1. Complex TPFS-F–HMPA (*1a*)

HMPA (452 μL, 2.6 mmol) was added to a solution of TPFS-F (950 mg, 1.73 mmol) in dichloroethane (5.2 mL) at 80 °C. The mixture was allowed to cool slowly to room temperature and kept for additional 16 h. The solvent was decanted, the crystals were washed with hexane, and dried in vacuum affording 854 mg of compound **1a** (68% yield). M.p. 125–140 °C. Due to the low solubility of the complex in $CDCl_3$, the NMR spectra were recorded just after addition of 1.0 equiv. of HMPA to a solution of TPFS-F in $CDCl_3$ (ca. 0.5 mol/L). NMR ^{1}H (200 MHz, $CDCl_3$, δ): 2.59 (d, 12H, $J = 9.3$); NMR ^{19}F (188 MHz, $CDCl_3$, δ): −160.1 (m, 6F, *meta*), −153.3 (br s, 1F, $\Delta\nu_{1/2} = 47.2$ Hz, Si–F), −145.7 (t, 3F, $J = 17.3$, *para*), −128.4 (br m, 6F, *ortho*).

4.2. Complex TPFS-Cl–HMPA (*1b*)

HMPA (465 μL, 2.4 mmol) was added to a stirred solution of TPFS-Cl (905 mg, 1.6 mmol) in dichloroethane (5.2 mL) at 50 °C. The stirring was stopped, the mixture was allowed to cool slowly to 5 °C and kept at this temperature for additional 16 h. The cold solvent was decanted, the crystals were washed with hexane, and dried in vacuum affording 1.034 g of compound **1b** (86% yield). M.p. 165–167 °C. Due to the low solubility of the complex in $CDCl_3$, the NMR spectra were recorded just after addition of 1.0 equiv. of HMPA to a solution of TPFS-Cl in $CDCl_3$ (ca. 0.5 mol/L). NMR ^{1}H (200 MHz, $CDCl_3$, δ): 2.53 (d, 12H, $J = 9.3$); NMR ^{19}F (188 MHz, $CDCl_3$, δ): −160.6 (m, 6F, *meta*), −147.3 (t, 3F, $J = 20.1$, *para*), −127.7 (d, 6F, $J = 19.4$, *ortho*).

4.3. Equimolar mixture of TPFS-F and NMP in $CDCl_3$ (ca. 0.5 mol/L)

NMR ^{1}H (200 MHz, $CDCl_3$, δ): 1.94–2.7 (m, 2H, CH_2), 2.36 (t, 2H, $J = 8.0$, CH_2), 2.82 (s, 3H, NMe), 3.38 (t, 2H, $J = 7.1$, CH_2); NMR ^{19}F (188 MHz, $CDCl_3$, δ): −159.9 (m, 6F, *meta*); −157.9 (br s, $\Delta\nu_{1/2} = 318.2$ Hz, 1F, Si–F), −145.2 (m, 3F, *para*), −128.3 (dm, 6F, $J = 19.4$, *ortho*).

4.4. Complex TPFS(HMPA)$_2^+$TfO$^-$ (*3a*)

HMPA (219 μL, 1.26 mmol) was added to a stirred solution of TPFS-OTf (408 mg, 0.6 mmol) in benzene (4 mL) at room temperature that caused the formation of a precipitate. The resulting suspension was heated with a bath of 80 °C and dichloroethane (3.5 mL) was added dropwise. When the mixture became homogeneous, the heating bath was removed, and the reaction flask was allowed to stand for 16 h at room temperature. The solvent was decanted, the crystals were washed with benzene, and dried in vacuum affording 370 mg of compound **3a** (60% yield). M.p. 196–200 °C.

4.5. Complex TPFS-NMP$^+$TfO$^-$ (*2b*)

NMP (58 μL, 0.6 mmol) was added to a stirred solution of TPFS-OTf (408 mg, 0.6 mmol) in benzene (2.4 mL) at room temperature. The resulting suspension was heated to effect dissolution (ca. 80 °C) and the mixture was allowed to slowly cool to room temperature and kept for additional 16 h. The solvent was decanted, the crystals were washed with benzene, and dried in vacuum affording 450 mg of compound **2b** (88% yield). M.p. 78–80 °C. NMR ^{1}H (200 MHz, $CDCl_3$, δ): 2.19–2.42 (br m, 2H, CH_2), 2.81 (br t, 2H, $J = 7.0$, CH_2), 3.24 (s, 3H, NMe), 3.97 (br t, 2H, $J = 6.0$, CH_2); NMR ^{13}C (50 MHz, $CDCl_3$, δ): 17.3, 31.3, 33.1, 54.1, 101.3 (tm, $J = 25.6$), 120.5 (q, $J = 320.4$, CF_3), 137.9 (dm, $J = 256.7$), 145.2 (dm, $J = 256.7$), 149.4 (dm, $J = 245.0$); 175.1; NMR ^{19}F (188 MHz, $CDCl_3$, δ): −158.9 (m, 6F, *meta*), −143.9 (t, 3F, $J = 20.0$, *para*), −127.0 (dm, 6F, $J = 19.6$, *ortho*), −80.4 (s, 3F, OTf); ^{29}Si NMR (59.6 MHz, $CDCl_3$, δ): −25.85.

4.6. Mixture of 1 equiv. TPFS-OTf and 2 equiv. NMP in $CDCl_3$ (ca. 0.5 mol/L) [complex TPFS(NMP)$_2^+$TfO$^-$ (*3b*)]

NMR ^{1}H (200 MHz, $CDCl_3$, δ): 2.12 (quint, 2H, $J = 7.5$, CH_2), 2.50 (t, 2H, $J = 7.5$, CH_2), 2.97 (s, 3H, NMe), 3.66 (t, 2H, $J = 7.5$, CH_2); NMR ^{13}C (50 MHz, $CDCl_3$, δ): 17.4, 30.7, 31.3, 51.8, 102.5 (tm, $J = 26.0$), 120.5 (q, $J = 319.5$, CF_3), 137.8 (dm, $J = 258.5$), 144.9

(dm, $J = 260.3$), 147.1 (dm, $J = 248.6$), 175.8; NMR ^{19}F (188 MHz, $CDCl_3$, δ): −159.2 (m, 6F, *meta*), −145.0 (tt, 3F, $J = 20.1$; 5.5, *para*), −127.6 (dm, 6F, $J = 19.4$, *ortho*), −80.2 (s, 3F, OTf); NMR ^{29}Si (59.6 MHz, $CDCl_3$, δ): −49.67.

4.7. 2-Tris(pentafluorophenyl)silyloxybenzaldehyde (4)

A solution of TPFS-Cl (2.00 g, 3.53 mmol) and pyridine (300 μL, 3.71 mmol) in CH_2Cl_2 (3.5 mL) was cooled to −20 °C. Salicyl aldehyde (431 mg, 3.71 mmol) was added dropwise, and after stirring for 5 min the cooling bath was removed. Suspension was stirred for additional 15 min and the solvent was evaporated in vacuum. The residue was extracted with hot hexane (50 °C) (3 × 7 mL). Combined extracts were slowly cooled to −23 °C and kept for 16 h at this temperature. The cold solvent was decanted, and the crystals were dried in vacuum affording 1.90 g of compound **4** (82% yield). M.p. 110–115 °C. NMR ^1H (200 MHz, $CDCl_3$, δ): 6.96 (d, 1H, $J = 7.7$, CH_{Ar}), 7.22 (t, 1H, $J = 7.7$, CH_{Ar}), 7.53 (td, 1H, $J = 7.7$, 1.8, CH_{Ar}), 7.74 (dd, 1H, $J = 7.7$, 1.8, CH_{Ar}), 9.99 (s, 1H, CH=O); NMR ^{13}C (75 MHz, $CDCl_3$, δ): 105.7 (tm, $J = 27.6$), 120.9, 123.8, 125.6, 132.3, 136.3, 137.1 (dm, $J = 254.9$), 143.9 (dm, $J = 259.8$), 149.3 (dm, $J = 248.2$), 153.5, 190.6; NMR ^{19}F (188 MHz, $CDCl_3$, δ): −160.7 (m, 6F, *meta*), −147.7 (tt, 3F, $J = 20.1$, 4.9, *para*), −128.7 (dm, 6F, $J = 18.7$, *ortho*); NMR ^{29}Si (60 MHz, $CDCl_3$, δ): −39.17.

4.8. N-[2-Tris(pentafluorophenyl)silyloxybenzoyl]-pyrrolidine (5)

Triethylamine (252 μL, 1.81 mmol) and *N*-(2-hydroxybenzoyl)pyrrolidine (329 mg, 1.72 mmol) were successively added to a suspension of TPFS-OTf (1.168 g, 1.72 mmol) in dichloroethane (7 mL) at 0 °C. After dissolution of starting amide TPFS-OTf (ca. 1–2 min) the reaction mixture became turbid. The mixture was filtered through glass wool, and the filtrate was kept for 16 h at 5 °C. The cold solvent was decanted, the crystals were washed twice with dichloroethane, and dried in vacuum affording 817 mg of compound **5** (66% yield). M.p. 132–134 °C. According to ^1H NMR the product contains ca. 10% of dichloroethane. The crystals for X-ray diffraction analysis were grown from benzene. NMR ^1H (200 MHz, $CDCl_3$, δ): 1.85–2.07 (m, 4H, $(CH_2)_2$), 3.45 (t, 2H, $J = 6.4$, NCH_2); 3.72 (t, 2H, $J = 6.4$, NCH_2), 6.80–7.13 (m, 2H, $2CH_{Ar}$), 7.28–7.52 (m, 2H, $2CH_{Ar}$); NMR ^{19}F (188 MHz, $CDCl_3$, δ): −162.5 (m, 6F, *meta*); −152.9 (tt, 3F, $J = 20.1$, 3.1, *para*), −130.2 (dm, 6F, $J = 18.7$, *ortho*).

4.9. N-Methyl-N-[2-tris(pentafluorophenyl)silyloxybenzyliden]amine (6)

N-Methyl-*N*-[2-hydroxybenzyliden]amine (270 mg, 2.0 mmol) was added dropwise to a solution of TPFS-Cl (1.13 g, 2.0 mmol) and NEt_3 (334 μL, 2.4 mmol) in CH_2Cl_2 (4.0 mL) at −20 °C. After 5 min of stirring the cooling bath was removed, the mixture was stirred for additional 5 min, and the solvent was evaporated in vacuum. The residue was extracted with boiling hexane (3 × 7 mL), the combined extracts were allowed to cool slowly to −25 °C and kept for 16 h at this temperature. The cold solvent was decanted, and the crystals were dried in vacuum affording 762 mg of compound **6** (59% yield). M.p. 142–144 °C. NMR ^1H (200 MHz, $CDCl_3$, δ): 3.14 (s, 3H, NMe), 6.79 (d, 1H, $J = 8.2$, CH_{Ar}), 7.13 (t, 1H, $J = 7.4$, CH_{Ar}), 7.36–7.51 (m, 2H, CH_{Ar}), 8.21 (s, 1H, N=CH); NMR ^{13}C (50 MHz, $CDCl_3$, δ): 45.8, 111.7 (tm, $J = 27.8$), 121.2, 121.9, 122.9, 131.3, 134.0, 137.4 (dm, $J = 245.3$), 142.5 (dm, $J = 247.4$), 148.2 (dm, $J = 244.2$), 153.7, 163.9; NMR ^{19}F (188 MHz, $CDCl_3$, δ): −161.6 (m, 6F, *meta*); −150.9 (t, 3F, $J = 20.1$, *para*); −129.0 (dm, 6F, $J = 19.4$, *ortho*); NMR ^{29}Si (60 MHz, $CDCl_3$, δ): −73.25.

4.10. (R*,R*)-2-[1-Tris(pentafluorophenyl)silyloxy-2-methylpropyl]cyclopentanone (7)

A solution of 1-tris(pentafluorophenyl)silyloxycyclopentene (440 mg, 0.72 mmol) and isobutyraldehyde (69 μL, 0.76 mmol) in dichloromethane (1.4 mL) was kept without stirring for three days at 5 °C. The cold solvent was decanted, the crystals were washed twice with hexane, and dried in vacuum affording 206 mg of compound **7** (42% yield). M.p. 104–114 °C. NMR ^1H (250 MHz, $CDCl_3$, δ): 0.86 (d, 3H, $J = 6.7$, CH_3), 0.97 (d, 3H, $J = 6.7$, CH_3), 1.43 (ddd, 1H, $J = 24.8$, 12.4, 6.1) and 1.68–2.41 (m, 6H) and 2.60 (dt, 1H, $J = 13.0$, 9.1) ($(CH_2)_3CH$ and $CHMe_2$), 3.81 (d, 1H, $J = 9.1$, CH–O); NMR ^{13}C (75 MHz, $CDCl_3$, δ): 14.2 (q, $J = 14.1$), 19.6 (q, $J = 14.7$), 20.0, 26.9, 31.5 (d, $J = 8.1$), 37.8, 51.4, 80.1, 107.5 (tm, $J = 28.8$), 137.2 (dm, $J = 253.2$), 143.1 (dm, $J = 256.5$), 148.8 (dm, J = 246.4), 221.2; NMR ^{19}F (188 MHz, $CDCl_3$, δ): −161.6 (m, 6F, *meta*), −149.9 (tt, 3F, $J = 20.3$, 4.5, *para*), −128.5 (dm, 6F, $J = 18.1$, *ortho*); NMR ^{29}Si (60 MHz, $CDCl_3$, δ): −40.89.

4.11. Complex 9 · Cl(CH2)2Cl

Succindiamide **8** (305 mg, 1.36 mmol) was added to a solution of TPFS-OTf (924 mg, 1.36 mmol) in dichloroethane (6.8 mL) at 80 °C. When the solution became homogeneous, the stirring was stopped, the mixture was allowed to cool slowly to 5 °C, and kept for 16 h at this temperature. The solvent was decanted, and the crystals were dried in vacuum affording 875 mg of compound **9** (64% yield). M.p. 90–100 °C. NMR ^1H (300 MHz, $CDCl_3$, δ): 1.99 (quint, 4H, $J = 6.8$, $2NCH_2CH_2$), 2.07 (quint, 4H, $J = 6.8$, $2NCH_2CH_2$), 3.08 (s, 4H, $C(CH_2)_2C$), 3.58 (t, 4H, $J = 6.7$, $2NCH_2$), 3.73 (s, 4H, $Cl(CH_2)_2Cl$), 3.74 (t, 4H, $J = 6.7$, $2NCH_2$); NMR ^{13}C (50 MHz, $CDCl_3$, δ): 24.3, 25.5, 28.4, 43.4 ($Cl(CH_2)_2Cl$), 48.0 (br, $\Delta\nu_{1/2} = 9.1$ Hz), 48.9 (br, $\Delta\nu_{1/2} = 8.6$ Hz), 173.1; NMR ^{19}F

Table 4
Crystallographic parameters of studied compounds

	1a	**1b**	**2b**	**3a**	TPFS-F	TPFS-Cl	**4**	**5**	**6**	**7**	**9**
Diffractometer	Smart APEX II	Smart APEX II	Smart APEX II	Smart 1000	Smart 1000	Smart 1000	Smart APEX II	Smart APEX II	Smart APEX II	Smart 1000	Smart APEX II
Molecular formula	$C_{24}H_{18}F_{16}N_3OPSi$	$C_{24}H_{18}ClF_{15}N_3OPSi$	$C_{30}H_{15}F_{18}NO_4SSi$	$C_{31}H_{36}F_{18}N_6O_5P_2SSi$	Ctextsubscript18$F_{16}Si$	$C_{18}ClF_{15}Si$	$C_{25}H_4F_{15}O_2Si$	$C_{29}H_{12}F_{15}NO_2Si$	$C_{26}H_8F_{15}NOSi$	$C_{27}H_{15}F_{15}O_2Si$	$C_{33}H_{24}Cl_2F_{18}N_2O_5SSi$
Formula weight	727.47	743.92	855.58	1036.75	548.27	564.72	649.37	719.49	663.42	684.48	1001.59
Dimension (mm)	0.1 × 0.1 × 0.02	0.08 × 0.08 × 0.08	0.05 × 0.05 × 0.02	0.2 × 0.1 × 0.1	0.07 × 0.07 × 0.01	0.25 × 0.20 × 0.15	0.4 × 0.4 × 0.2	0.15 × 0.1 × 0.1	0.05 × 0.04 × 0.01	0.1 × 0.05 × 0.05	0.03 × 0.03 × 0.01
Crystal system	Monoclinic	Monoclinic	Triclinic	Monoclinic	Orthorhombic	Monoclinic	Monoclinic	Orthorhombic	Orthorhombic	Triclinic	Monoclinic
Space group	$P2_1/n$	$P2_1/n$	$P\bar{1}$	$P2_1/c$	$Pna2_1$	$P2_1/c$	$P2_1/n$	$P2_12_12_1$	$Pbca$	$P\bar{1}$	$P2_1/c$
a (Å)	9.7483(5)	a = 9.917(1)	11.4751(7)	12.1721(18)	9.414(4)	9.532(4)	16.3756(14)	8.6483(4)	12.0132(5)	9.190(2)	20.928(3)
b (Å)	17.9256(8)	17.793(2)	16.879(1)	16.055(2)	17.631(8)	26.181(12)	8.5564(7)	16.4559(8)	18.9155(7)	11.370(2)	11.390(2)
c (Å)	15.8298(7)	15.959(2)	17.052(1)	21.577(3)	10.752(5)	7.643(4)	17.7576(15)	19.2543(9)	20.8174(8)	14.674(3)	32.380(5)
α (°)			98.680(1)							93.724(4)	
β (°)	93.940(1)	94.571(4)	98.831(1)	97.578(3)		98.035(9)	113.060(2)			94.201(4)	90.285(3)
γ (°)			96.278(1)							100.554(4)	
V (Å^3)	2759.6(2)	2807.0(5)	3196.5(4)	4180(1)	1785(1)	1889(2)	2289.3(3)	2740.2(2)	4730.5	1498.5(5)	4016
Z	4	4	4	4	4	4	4	4	8	2	8
ρ_{calc} (g cm^{-1})	1.751	1.760	1.778	1.647	2.041	1.986	1.884	1.744	1.863	1.517	1.724
Temperature (K)	100	100	100	120	120	120	100	100	100	120	100
Maximum Θ (°)	28.01	30.03	30.03	30.02	30.10	30.02	30.59	31.93	27.	27.88	26.02
Scan type	ω/φ	ω/φ	ω/φ	ω/φ	ω/φ	ω/φ	ω/φ	ω/φ	ω/φ	ω/φ	
Radiation, λ(Mo Kα) (Å)	0.71073	0.71073	0.71073	0.71073	0.71073	0.71073	0.71073	0.71073	0.71073	0.71073	0.71073
Linear absorption (μ), cm^{-1}	2.79	3.63	2.84	3.11	3.01	4.17	2.51	2.20	2.43	1.96	3.86
T_{min}/T_{max}	0.994/0.963	0.972/0.972	0.986/0.994	0.970/0.930	0.997/ 0.969	0.940/ 0.893	0.952/0.896	0.978/0.958	0.998/0.978	0.990/0.971	0.996/0.989
F(000)	1456	1488	1704	2104	1064	1096	1276	1432	2624	684	4016
Total reflections (R_{int})	26230	23271	41762	48804	13891	24598	26561	39385	45153	10904	71999
Number of independent reflections	6636	8167	18624	12167	5147	5504	7031	9460	5232	7104	15099
Number of independent reflections with $I > 2(\alpha)$	4859	5711	10315	9041	4658	3680	3554	8765	4019	5247	5538
Parameters	421	421	993	589	317	316	388	433	398	408	1084
wR_2	0.0957	0.1036	0.0981	0.0960	0.0850	0.1037	0.1476	0.0769	0.0932	0.1203	0.2048
R_1	0.0403	0.0413	0.045	0.0390	0.0306	0.0419	0.0556	0.0292	0.0344	0.0508	0.0807
Goodness-of-fit	1.028	1.011	0.985	1.025	1.005	0.972	0.984	1.022	1.003	0.981	0.958
ρ_{max}/ρ_{min} (e Å^{-3})	0.732/−0.336	0.565/−0.488	0.794/−0.436	0.462/−0.506	0.288/−0.243	0.599/−0.307	0.681/−0.313	0.366/−0.221	0.320/−0.259	0.482/−0.318	0.560/−0.479

(282 MHz, $CDCl_3$, δ): −160.5 (m, 6F, *meta*), −147.4 (tt, 3F, $J = 20.1$, 4.2, *para*), −128.7 (dm, 6F, $J = 19.7$, *ortho*), −79.2 (s, 3F, OTf).

4.12. Tris(pentafluorophenyl)silyloxybenzene

Phenol (224 g, 2.38 mmol) was added in one portion to a solution of TPFS-Cl (1.35 g, 2.38 mmol) and pyridine (202 μL, 2.5 mmol) in CH_2Cl_2 (2.5 mL) at −20 °C. After stirring for 10 min the cooling bath was removed, the mixture was stirred for additional 10 min and then concentrated in vacuum. The residue was extracted with hexane (5 mL and 2 × 3 mL), the combined extracts were concentrated in vacuum, and the residual oil was distilled to afford 1.10 g of colorless viscous oil (74% yield). B.p. 160–170 °C (bath temperature)/1.1 Torr. NMR ^1H (300 MHz, $CDCl_3$, δ): 6.90 (d, 2H, $J = 8.1$, $2CH_{Ar}$); 7.08 (t, 1H, $J = 7.5$, CH_{Ar}); 7.23–7.31 (m, 2H, $2CH_{Ar}$); NMR ^{13}C (75 MHz, $CDCl_3$, δ): 104.4 (tm, $J = 13.3$), 119.1, 123.6, 129.8, 137.6 (dm, $J = 254.9$), 144.3 (dm, $J = 259.8$), 149.3 (dm, $J = 248.2$), 152.3; NMR ^{19}F (282 MHz, $CDCl_3$, δ): −160.2 (m, 6F, *meta*), −146.6 (tt, 3F, $J = 19.5$, 5.2, *para*), −127.7 (dm, 6F, $J = 18.2$, *ortho*); NMR ^{29}Si (60 MHz, $CDCl_3$, δ): −35.98.

4.13. Computational details

The quantum chemical calculations of structures **1a**,**b**, **3a** and **5** in the crystal were carried out using the VASP 4.6.28 code [38]. Conjugated gradient technique was used for optimizations of the atomic positions (started from experimental data) and minimization of total energy. Projected augmented wave (PAW) method was applied to account for core electrons while valence electrons were approximated by plane-wave expansion with 400 eV cutoffs [38]. Exchange and correlation terms of total energy were described by PBE [39] exchange-correlation functional. Kohn–Sham equations were integrated using Γ-point approximation. We believe that Γ-point approximation is sufficient for **1a**,**b**, **3a**, and **5** because of their large crystal unit cells. Using DFT method it is not possible to take into account dispersion interactions. For this reason calculated cell parameters may be systematically overestimated or underestimated up to 5%. Thus, the experimental values of cell parameters were used in the calculations. At a final step of our calculations atomic displacements converged were better than 0.02 eV $Å^{-1}$, as well as energy variations were less than 10^{-3} eV. In order to carry out the topological analysis of electron density distribution function in terms of Bader's theory "Atoms in molecules" (AIM) [22], the dense FFT (fast Fourier transformation) grid was used (corresponding to cutoff 1360 eV). The latter was obtained by separate single point calculation of optimized geometry with hard PAWs for each atom type. The topological analysis of electron density distribution function was carried out using AIM program – part of ABINIT software package [40].

One of the useful advantages of AIM theory is the possibility to evaluate the energy of closed shell interactions, as well as interactions of intermediate type, using correlation formula proposed by Espinosa et al. [26]:

$$E_{A-B} \approx -1/2V^e(r)$$

where E_{A-B} is the energy of weak interatomic contacts or coordination bond and $V^e(r)$ is potential energy density in CP(3, −1). The value of $V^e(r)$ can be calculated from values $\rho(r)$ and $\nabla^2\rho(r)$ in CP(3, −1) using Kirzhnitz formula for kinetic energy density and local virial theorem expression [41]. We utilized this methodological background for detailed analysis of the influence of the crystal packing on geometry and electron structure.

4.14. X-ray crystallographic study

All X-ray diffraction measurements were carried out with a SMART 1000 CCD and Smart APEX II diffractometers. The frames were integrated and corrected for absorption by the SAINT and SADABS programs [42]. The details of crystallographic data and experimental conditions are presented in Table 4. Important structural parameters are summarized in Tables 1 and 3.

The structures were solved by the direct method and refined by full-matrix least-squares technique against F^2 in the anisotropic–isotropic approximation. The hydrogen atoms were located from difference electron density syntheses and refined in rigid body model. All calculations were performed using the SHELXTL PLUS 5.10 program package [43].

Analysis of Fourier maps in structure **9** allowed one to reveal about 8–10 peaks of residual electron density (1.2–3.1 e A^{-3}) in cavities between organosilicon cations. These peaks can be considered as superposition of several $C_2H_4Cl_2$ molecules with different occupation values. We could not established appropriate model for refining of the above residual electron density. Thus, we had to exclude unresolved solvent by means of SQUEEZE procedure [44]. The similar problem occurred in structure **7** and it was solved analogously.

Acknowledgements

This work was supported by the Ministry of Science (Projects MK-4483.2007.3 and MK-3894.2007.3), the Russian Foundation for Basic Research (Project 08-03-00560) and Russian Academy of Sciences (Program # 8).

Appendix A. Supplementary material

CCDC 665556, 665557, 665558, 665559, 665560, 665561, 665562, 665563, 665564, 665565 and 665566 contain the supplementary crystallographic data for this paper. These data can be obtained free of charge from The Cambridge Crystallographic Data Centre via www.ccdc.cam.ac.uk/data_request/cif. Supplementary data associated with

this article can be found, in the online version, at doi:10.1016/j.jorganchem.2007.12.022.

References

[1] (a) C. Chuit, R.J.P. Corriu, C. Reye, J.C. Young, Chem. Rev. 93 (1993) 1371;
(b) D. Kost, I. Kalikhman, in: Y. Apeloig, Z. Rappoport (Eds.), The Chemistry of Organic Silicon Compounds, vol. 2, Wiley, Chichester, UK, 1998, p. 1339;
(c) R.R. Holmes, Chem. Rev. 96 (1996) 927.

[2] (a) W.J. Middleton, Org. Synth. 64 (1986) 221;
(b) C.J. Handy, Y.-F. Lam, P. DeShong, J. Org. Chem. 65 (2000) 3542.

[3] (a) K.D. Onan, A.T. McPhail, C.H. Yoder, R.W. Hillyard Jun., J. Chem. Soc., Chem. Commun. (1978) 209;
(b) A.A. Macharashvili, V.E. Shklover, Yu.T. Struchkov, G.I. Oleneva, E.P. Kramarova, A.G. Shipov, Yu.I. Baukov, J. Chem. Soc., Chem. Commun. (1988) 683;
(c) D. Kost, I. Kalikhman, Adv. Organomet. Chem. 50 (2004) 1.

[4] (a) A.D. Dilman, P.A. Belyakov, A.A. Korlyukov, M.I. Struchkova, V.A. Tartakovsky, Org. Lett. 7 (2005) 2913;
(b) A.D. Dilman, V.V. Levin, M. Karni, Y. Apeloig, J. Org. Chem. 71 (2006) 7214;
(c) A.D. Dilman, V.V. Levin, P.A. Belyakov, M.I. Struchkova, V.A. Tartakovsky, Synthesis (2006) 447;
(d) V.V. Levin, A.D. Dilman, P.A. Belyakov, A.A. Korlyukov, M.I. Struchkova, M.Y. Antipin, V.A. Tartakovsky, Synthesis (2006) 489;
(e) A.D. Dilman, D.E. Arkhipov, P.A. Belyakov, M.I. Struchkova, V.A. Tartakovsky, Russ. Chem. Bull. 55 (2006) 517;
(f) A.D. Dilman, V.V. Gorokhov, P.A. Belyakov, M.I. Struchkova, V.A. Tartakovsky, Tetrahedron Lett. 47 (2006) 6217;
(g) V.V. Levin, A.D. Dilman, P.A. Belyakov, M.I. Struchkova, V.A. Tartakovsky, Tetrahedron Lett. 47 (2006) 8959;
(h) V.V. Levin, A.D. Dilman, P.A. Belyakov, A.A. Korlyukov, M.I. Struchkova, V.A. Tartakovsky, Mendeleev Commun. (2007) 105.

[5] A.R. Bassindale, T. Stout, Tetrahedron Lett. 26 (1985) 3403.

[6] (a) V.A. Bain, R.C.G. Killean, M. Webster, Acta Crystallogr., Sect. B 25 (1969) 156;
(b) O. Bechstein, B. Ziemer, D. Hass, S.I. Troyanov, V.B. Rybakov, G.N. Maso, Z. Anorg. Allg. Chem. 582 (1990) 211;
(c) For recent comprehensive study of interaction of $RSiF_3$ with pyridines see: M. Nakash, D. Gut, M. Goldvaser, Inorg. Chem. 44 (2005) 1023.

[7] (a) H. Emde, D. Domsch, H. Feger, U. Frick, A. Gotz, H.H. Hergott, K. Hofmann, W. Kober, K. Krageloh, T. Oesterle, W. Steppan, W. West, G. Simchen, Synthesis (1982) 1;
(b) G. Simchen, in: G.L. Larson (Ed.), Advances in Silicon Chemistry, vol. 1, JAI Press, Inc., Greenwich, CT, 1991, p. 189.

[8] A.D. Dilman, S.L. Ioffe, Chem. Rev. 103 (2003) 733.

[9] M. Arshadi, D. Johnels, U. Edlund, C.-H. Ottosson, D. Cremer, J. Am. Chem. Soc. 118 (1996) 5120.

[10] V.V. Levin, A.D. Dilman, P.A. Belyakov, A.A. Korlyukov, M.I. Struchkova, V.A. Tartakovsky, Tetrahedron Lett. 46 (2005) 3729.

[11] E. Hey-Hawkins, U. Dettlaff-Weglikowska, D. Thiery, H.G. von Schnering, Polyhedron 11 (1992) 1789.

[12] C. Leis, D.L. Wilkinson, H. Handwerker, C. Zybill, G. Muller, Organometallics 11 (1992) 514.

[13] H. Kobayashi, K. Ueno, H. Ogino, Chem. Lett. 28 (1999) 239.

[14] C. Zybill, G. Müller, Angew. Chem., Int. Ed. Engl. 26 (1987) 669.

[15] C. Zybill, D.L. Wilkinson, G. Müller, Angew. Chem., Int. Ed. Engl. 27 (1988) 583.

[16] F.H. Allen, O. Kennard, D.G. Watson, L. Brammer, A.G. Orpen, R. Taylor, J. Chem. Soc., Perkin. Trans. II (1987) S1.

[17] H.B. Bürgi, V. Shklover, in: H.B. Bürgi, J.D. Dunitz (Eds.), Structure Correlation, vol. 1, VCH Publishers, New York, 1994, p. 303.

[18] Cambridge Structural Database, Release, 2007.

[19] (a) K. Hensen, M. Kettner, M. Bolte, Acta Crystallogr., Sect C 54 (1998) 358;
(b) K. Hensen, T. Zengerly, T. Muller, P. Pickel, Z. Anorg. Allg. Chem. 588 (1988) 21.

[20] S.S. Karlov, D.A. Tyurin, M.V. Zabalov, A.V. Churakov, G.S. Zaitseva, J. Mol. Struct. Theochem 724 (2005) 31.

[21] A.A. Korlyukov, K.A. Lyssenko, M.Yu. Antipin, Russ. Chem. Bull. 51 (2002) 1423.

[22] R.F.W. Bader, Atoms In molecules. A Quantum Theory, Clarendron Press, Oxford, 1990.

[23] N. Kocher, J. Henn, B. Gostevskii, D. Kost, I. Kalikhman, B. Engels, D. Stalke, J. Am. Chem. Soc. 126 (2004) 5563.

[24] A.A. Korlyukov, S.A. Pogozhikh, Yu.E. Ovchinnikov, K.A. Lyssenko, M.Yu. Antipin, A.G. Shipov, O.A. Zamyshlyaeva, E.P. Kramarova, Vad.V. Negrebetsky, I.P. Yakovlev, Yu.I. Baukov, J. Organomet. Chem. 691 (2006) 3962.

[25] V.V. Levin, A.D. Dilman, A.A. Korlyukov, P.A. Belyakov, M.I. Struchkova, M.Yu. Antipin, V.A. Tartakovsky, Russ. Chem. Bull. 56 (2007) 1394.

[26] E. Espinosa, E. Mollins, C. Lecomte, Chem. Phys. Lett. 285 (1998) 170.

[27] A.A. Korlyukov, E.A. Komissarov, M.Yu Antipin, N.V. Alekseev, K.V. Pavlov, O.V. Krivolapova, V.G. Lahtin, E.A. Chernyshev, J. Mol. Struct., doi:10.1016/j.molstruc.2007.04.019.

[28] J.I. Musher, Angew. Chem., Int. Ed. Engl. 8 (1969) 54.

[29] The crystal structures containing interaction of aldehyde with silicon Lewis acids are not described. However, in solution the interaction of Me_3SiNTf_2 with crotonaldehyde was observed at −40 °C, see: B. Mathieu, L. Ghosez, Tetrahedron 58 (2002) 8219.

[30] Earlier we observed that $(C_6F_5)_3Si$-group forms short covalent Si–O, Si–C, and Si–N bonds, see Refs. [4a,4d], and A.D. Dilman, D.E. Arkhipov, A.A. Korlyukov, V.P. Ananikov, V.M. Danilenko, V.A. Tartakovsky, J. Organomet. Chem. 690 (2005) 3680.

[31] Y. Wan, J.G. Verkade, Organometallics 13 (1994) 4164.

[32] K. Chenoweth, S. Cheung, A.C.T. van Duin, W.A. Goddard III, E.M. Kober, J. Am. Chem. Soc. 127 (2005) 7192.

[33] H.-J. Frohn, A. Lewin, V.V. Bardin, J. Organomet. Chem. 568 (1998) 233.

[34] V.V. Levin, A.D. Dilman, P.A. Belyakov, A.A. Korlyukov, M.I. Struchkova, V.A. Tartakovsky Eur. J. Org. Chem. (2004) 5141.

[35] W.L. Mock, D.C.Y. Chua, J. Chem. Soc., Perkin Trans. II (1995) 2069.

[36] T.M. Kitson, G.H. Freeman, Bioorg. Chem. 21 (1993) 354.

[37] M. Gay, A.M. Montana, V. Moreno, M. Font-Bardia, X. Solans, J. Organomet. Chem. 690 (2005) 4856.

[38] (a) G. Kresse, J. Hafner, Phys. Rev. B 47 (1993) 558;
(b) G. Kresse, Thesis, Technische Universitat Wien, 1993;
(c) G. Kresse, J. Furthmuller, Comput. Mat. Sci. 6 (1996) 15;
(d) G. Kresse, J. Furthmuller, Phys. Rev. B 54 (1996) 11169.

[39] J.P. Perdew, S. Burke, M. Ernzerhof, Phys. Rev. Lett. 77 (1996) 3865.

[40] X. Gonze, J.-M. Beuken, R. Caracas, F. Detraux, M. Fuchs, G.-M. Rignanese, L. Sindic, M. Verstraete, G. Zerah, F. Jollet, M. Torrent, A. Roy, M. Mikami, Ph. Ghosez, J.-Y. Raty, D.C. Allan, Comput. Mater. Sci. 25 (2002) 478.

[41] Yu.A. Abramov, Acta Crystallogr., Sect A 53 (1997) 264.

[42] Program SAINT, Bruker-AXS Inc., Madison, WI, USA, 2005;
G.M. Sheldrick, SADABS, v.2.01 Bruker/Siemens Area Detector Absorption Correction.

[43] G.M. Sheldrick, SHELXTL-97 V5.10, Bruker AXS, Madison, WI-53719, USA, 1997.

[44] A.L. Spek, J. Appl. Cryst. 36 (2003) 7.